DALTON
FULL PAPER

Synthesis, X-ray characterization and single molecule magnetic behaviour of $[Mn_{12}O_{12}(O_2CCH_2X)_{16}(H_2O)_4]\cdot m CH_2Cl_2\cdot n H_2O$ (1: X = Cl, $m = 2$, $n = 6$; 2: X = Br, $m = 4$, $n = 0$)†

Jin An,[a,b] Zhi-Da Chen,[a] Xi-Xiang Zhang,[c] Helgard G. Raubenheimer,*[b] Catharine Esterhuysen,[b] Song Gao[a] and Guang-Xian Xu[a]

[a] *The State Key Laboratory of Rare Earth Materials Chemistry and Applications, College of Chemistry and Molecular Engineering, Peking University, Beijing 100871, P.R. China*
[b] *Department of Chemistry, University of Stellenbosch, Private Bag X1, Matieland, 7602, South Africa. E-mail: hgr@maties.sun.ac.za; Fax: +27 21 808 3849; Tel: +27 21 808 3850*
[c] *Department of Physics, University of Science and Technology, Clear Water Bay, Hong Kong, P.R. China*

Received 14th June 2001, Accepted 18th September 2001
First published as an Advance Article on the web 24th October 2001

Two new complexes, **1** and **2**, with halo acetate ligands have been prepared from the reaction of $ClCH_2CO_2H$ or $BrCH_2CO_2H$ with the precursor Mn12Ac, and their structures and magnetic properties studied. The structures of complexes **1** and **2** consist of a central cubane-like $[Mn_4O_4]^{8+}$ unit held within a non-planar ring of eight Mn(III) ions by eight μ_3-O ions, sixteen $XCH_2CO_2^-$ units and four terminal water molecules, as well as included CH_2Cl_2 and H_2O. Different arrangements of the four Mn(IV) atoms relative to the eight Mn(III) atoms in the title complexes and other comparable complexes could play a role in the observed magnetic properties. Five and three periodic steps in the magnetic hysteresis loops are observed for both **1** and **2** at 2.2 and 2.6 K, respectively. $\chi'_m T$ values for complexes **1** and **2**, where χ'_m is the in-phase component of the AC magnetic susceptibility, exhibit a plateau in the 6–20 K region, below which there is an abrupt decrease in $\chi'_m T$. Their χ''_m signals measured at different frequencies are observed in the region 2–10 K, and exhibit a frequency dependency on the χ''_m AC peaks, with a predominant peak in the 4–10 K region. For these complexes, there is a difference between the zero-field-cooled (ZFC) and the field-cooled (FC) magnetization due to slow relaxation of the magnetization.

Introduction

Research on molecular magnetism has been expanding rapidly in the last few years, and particularly the study of large molecular clusters of metal ions has attracted extensive attention.[1] Nanoscale magnetic particles are expected to exhibit simultaneous classical and quantum behaviors. Mn12 nanomagnets serve as a prototype system for quantum tunneling. The first detailed results on the magnetization of Mn12Ac (twelve manganese atoms linked by acetate ligands) were reported in 1996.[2] In recent years, many theorists and experimentalists have focused on the unusual magnetic properties of such complexes.[3–7] Steps observed in the magnetic hysteresis loops of Mn12 nanomagnets are interpreted as evidence for thermally-assisted, field-tuned resonant tunneling between quantum spin states in a large number of identical high-spin molecules.

The largest number of steps, namely seven, has been observed for the complex Mn12Ac.[2] For analogous dodecanuclear manganese complexes, varying numbers of steps have been detected. Apart from Mn12Ac, other dodecanuclear manganese complexes with ligands derived from benzoic acids have also been studied. A few of these have been characterized by X-ray diffraction and the number of steps in their magnetic hysteresis loops identified.[8–10] A third family of molecules is the reduced anionic Mn12 complexes with half-integer ground states.[11,12] The reported hysteresis loops measured for these complexes exhibit one step accompanying the magnetization.[13]

We report herein two new analogues of Mn12 dodecanuclear manganese complexes, **1** and **2** (see title), with different halogen-substituted acetate ligands, $ClCH_2CO_2^-$ and $BrCH_2CO_2^-$. Both complexes were characterized by X-ray diffraction, and studied using a variety of magnetic experiments. Five and three steps were seen in their hysteresis loops at 2.2 and 2.6 K respectively.

Experimental

General

All chemicals and solvents were used as received. Yields were calculated from the stoichiometric reactions. All preparations and manipulations were performed under aerobic conditions. $[Mn_{12}O_{12}(CH_3CO_2)_{16}(H_2O)_4]\cdot 2CH_3CO_2H\cdot 4H_2O$ was prepared according to a literature procedure.[14]

Syntheses

$[\{Mn_{12}O_{12}(O_2CCH_2Cl)_{16}(H_2O)_4\}\cdot 2CH_2Cl_2\cdot 6H_2O]$ 1. To a slurry of $[Mn_{12}O_{12}(CH_3CO_2)_{16}(H_2O)_4]\cdot 2CH_3CO_2H\cdot 4H_2O$ (0.50 g, 0.25 mmol) in CH_2Cl_2 (50 ml) was added $ClCH_2CO_2H$ (0.79 g, 8.0 mmol). The mixture was stirred for 24 h and filtered to remove a small amount of undissolved solid. Hexane (150 ml) was added to the filtrate until precipitation of a brown solid was observed, and the solution was stored overnight in a refrigerator. The resulting solid was collected by filtration and the

---

† Electronic supplementary information (ESI) available: rotatable 3-D crystal structure diagrams in CHIME format; tables of selected bond distances and angles for **1** and **2**; plots of magnetization data for **2**. See http://www.rsc.org/suppdata/dt/b1/b105258f/

DOI: 10.1039/b105258f

Table 1 Crystal data and structure refinement for complexes **1** and **2**

Complexes	**1**	**2**
Formula	$C_{34}H_{48}Cl_{20}Mn_{12}O_{54}$	$C_{36}H_{48}Br_{16}Cl_8Mn_{12}O_{48}$
M	2689.015	3470.18
T/K	173(2)	173(2)
Crystal system	Monoclinic	Tetragonal
Space group	$C2/c$	$I4_1/a$
a/Å	25.132(2)	26.647(4)
b/Å	13.195(2)	26.647(4)
c/Å	26.068(2)	12.850(3)
a/°	90.000	90.000
β/°	94.255(2)	90.000
γ/°	90.000	90.000
V/Å^3	8620.8(16)	9124(3)
Z	4	4
μ/mm^{-1}	2.394	8.929
Reflections collected	17900	23936
Unique reflections, R_{int}	8453, 0.0495	5156, 0.0793
R [$I > 2\sigma(I)$]	0.0573	0.0740
wR_2 (all data)	0.1735	0.2241

above treatment was repeated. Black micro-crystals of the complex **1** were collected by filtration, washed with hexane and diethyl ether, and dried in air, (yield 0.339 g, 31.5%). (Found: C, 16.11; H, 1.76%. Calc. for $C_{34}H_{48}Cl_{20}Mn_{12}O_{54}$ C, 15.17, H, 1.78%). $\tilde{\nu}_{max}$/cm^{-1} 3433br (coordinated H_2O), 1610vvs [ν(C=O) of bridge acetate group], 1431vvs [$\delta(CH_2)$ of CH_2Cl_2], 799s [ν(CCl) of CH_2Cl_2].

[{$Mn_{12}O_{12}(O_2CCH_2Br)_{16}(H_2O)_4$}·$4CH_2Cl_2$] 2. Micro-crystals of complex **2** were obtained using the same procedure as for complex **1** ($BrCH_2COOH$ was added), (yield 0.31 g, 22.3%). (Found: C, 12.45; H, 1.70%. Calc. for $C_{36}H_{48}Br_{16}Cl_8Mn_{12}O_{48}$ C, 12.45; H, 1.38%). $\tilde{\nu}_{max}$/cm^{-1} 3430br (coordinated H_2O), 1603sh [ν(C=O) of bridge acetate group], 1431vvs [$\delta(CH_2)$ of CH_2Cl_2], 946s [ν(CCl) of CH_2Cl_2].

Physical measurements

Analysis of C, H and N was carried out on a Carlo Erba 1106 instrument. Infrared spectra (400–4000 cm^{-1}) were recorded from KBr pellets on a Nicolet 7199B spectrophotometer. The alternating current magnetic susceptibility measurements and the magnetization *vs.* applied magnetic field at different temperatures (2.2 and 2.6 K) were carried out on a Quantum Design SQUID magnetometer, MPMS-5S for complexes **1** and **2**. Pascal's constants were used for the diamagnetic corrections.

X-Ray crystallography and structure solution for complexes 1 and 2

Complex 1. Recrystallization from CH_2Cl_2–hexane gave crystals suitable for X-ray structure analysis. Diffraction data for a black crystal of complex **1** were collected at 173 K on a Nonius Kappa CCD diffractometer with graphite monochromated Mo-Kα radiation (λ = 0.71073 Å) using φ and ω scans to fill the Ewald sphere (Nonius COLLECT[15]). Details of the data collection and structural refinement are summarized in Table 1. Empirical absorption corrections were performed using SCALEPACK.[16] The structure was solved by direct methods. All non-hydrogen atoms were refined anisotropically by full-matrix least-squares methods. The chlorine atoms were found to be highly disordered (both static and dynamic disorder were observed). Disordered positions were identified from the difference Fourier map and refined anisotropically, with the total site occupancy factor restrained to 1. C–Cl bond lengths were restrained to reasonable values. Furthermore, one of the three solvent water molecules was also found to be disordered over two positions, which were identified from the difference Fourier map and refined anisotropically with a total site occupancy factor of 1. The hydrogen atoms on two of the coordinated waters [O(8) and its symmetry equivalent, O(8)′] were located from the difference Fourier map. All calculations were performed using SHELX-97[17] within the WinGX package.[18] Figures were generated using Ortep3 for Windows.[19] Selected bond lengths and angles are given in the ESI.

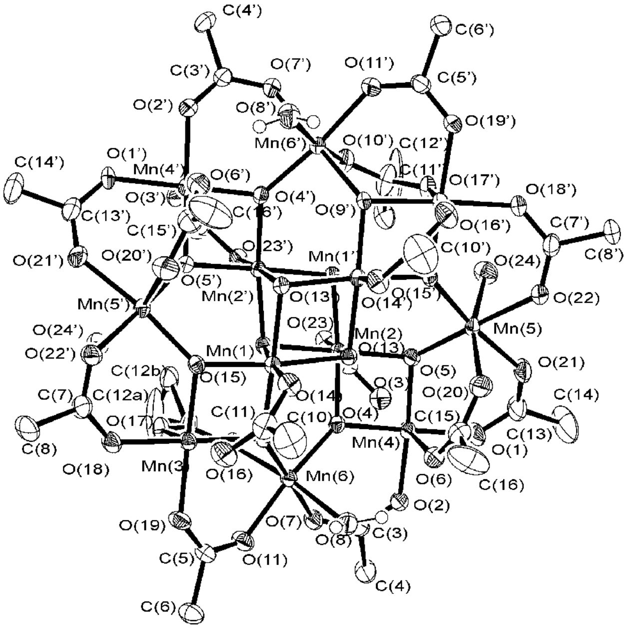

Fig. 1 Molecular structure of complex **1** showing the numbering scheme. For clarity, solvent molecules and chlorine atoms of the chloroacetate ligands are not shown. The O(8) and O(24) atoms correspond to the H_2O ligands.

Complex 2. Diffraction data for a black crystal of complex **2** were collected similarly to complex **1**. Details of the data collection and structural refinement are summarized in Table 1. Cylindrical absorption corrections were performed.[20] The crystal structure was solved by direct methods. The bromine atoms were found to be disordered, as the chlorine atoms were in the structure of complex **1**, and were dealt with in the same manner. C–Br bond lengths were restrained to reasonable values. Positions for the hydrogen atoms on the β-C atoms of the carboxylate ligands were calculated with bond distances of 0.97 Å. All calculations were performed using SHELX-97[17] within the WinGX package.[18] Figures were generated using Ortep3 for Windows.[19] Selected bond distances and angles are given in the ESI.

CCDC reference numbers 165981 and 165982.

See http://www.rsc.org/suppdata/dt/b1/b105258f/ for crystallographic data in CIF or other electronic format.

Results and discussion

Synthesis and structural studies

Synthesis. Complexes **1** and **2** were prepared according to a standard substitution procedure. In order to substitute the acetate ligands completely in the Mn12Ac precursor, an excess of the halo acetate ligands was used. The molar ratio of Mn12Ac to ligands was 1 to 32 for both reactions. To ensure complete substitution, the procedure was repeated.

Molecular structure of complex 1. The molecular structure of complex **1** is shown in Fig. 1. The two halves of the molecular structure are related to each other across a two-fold rotation axis, which runs through the center of the cluster. The skeleton consists of a cubane-like central core surrounded by the cations coordinated to the Mn(III) and Mn(IV) atoms, as has been previously described.[8–10,13,14,21,22]

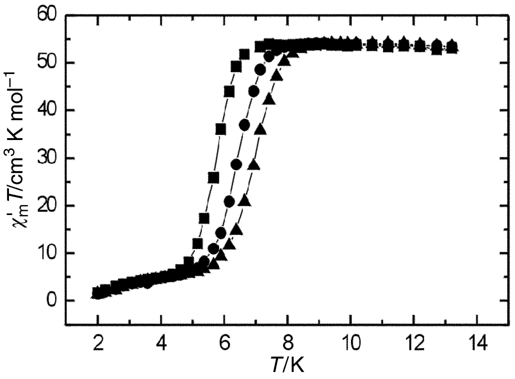

Fig. 2 Temperature dependence of χ'_mT for a polycrystalline sample of complex **1**, where χ'_m is the real component of the molar magnetic susceptibility measured in a zero DC field and 1.0 Oe AC field at three frequencies: (■) 133 (●) 1333 (▲) 9333 Hz.

Molecular structure of complex 2. The crystal structure of complex **2** has also been determined from X-ray diffraction data. The molecular structure is not shown, as it is very similar to that of complex **1**. The greatest difference is that complex **2** contains bromoacetate ligands as opposed to the chloroacetate ligands in **1**. Its structural skeleton is thus similar to complex **1**. The molecule also has a slightly higher symmetry, with a four-fold axis of symmetry (rather than the two-fold axis in **1**) relating the four quarters of the molecule to each other.

A comparison of complexes **1**, **2** and **3** (the structure of **3**—consisting of discrete dodecanuclear $[Mn_{12}O_{12}(3\text{-Cl-}C_6H_4CO_2)_{16}(3\text{-Cl-}C_6H_4CO_2H)(H_2O)_3]$ molecules—has been reported elsewhere)[10] shows that the peripheral ligations are different. All three complexes contain sixteen η^2-μ-carboxylate ligands, however, complex **3** contains three waters as well as one terminal $3\text{-Cl-}C_6H_4CO_2H$ ligand, whereas complexes **1** and **2** each contain four coordinated water molecules. In complex **3**, the four terminal ligands have a 1 : 1 : 2 arrangement, as compared to the 1 : 1 : 1 : 1 arrangement of the four terminal water molecules in complexes **1** and **2**. Previously reported Mn12 complexes have either three or four peripheral water molecules as terminal ligands, which are arranged in 1 : 1 : 1 : 1, 1 : 1 : 2 or 2 : 2 configurations.[8,9,13,21,22]

Crystal structures of complexes 1 and 2. The packing in complexes **1** and **2** is very similar, and can best be described by viewing the individual molecules as slightly flattened discs, with the cubane at the center. In both complexes **1** and **2**, the discs lie in alternating layers with the flattened sides parallel to each other, perpendicular to the unique axis (*b* in **1** and *c* in **2**). A zig-zag pattern of pairs of alternating molecules is observed if the crystal is viewed along the *c* axis in **1** and along both the *a* and *b* axes in complex **2**. In the *c* direction in complex **1**, the molecules are arranged in a zig-zag pattern of strings.

Magnetic properties

(Figures in this paper illustrate the magnetic properties of complex **1** only. Similar figures for complex **2** are included in the ESI.)

Alternating current magnetic susceptibility. In Fig. 2, the alternating current magnetic susceptibility measured in a zero DC field and 1.0 Oe AC field at three frequencies is plotted against temperature. The AC magnetic susceptibility data for complexes **1** and **2** indicated a relaxation process associated with the magnetization. A systematic frequency dependence at low temperature and a "two-step" decrease in the χ'_mT values was obtained. These results were further confirmed by the plot of the out-of-phase susceptibility, χ''_m, *versus* temperature in Fig. 3. One of the two relaxation processes occurs in the 2–4 K region and the other at 4–10 K. The plateau values for complexes **1** and **2** appear at $\chi'_mT \cong 52$ cm^3 K mol^{-1} and $\chi'_mT \cong 53$ cm^3 K mol^{-1} in the range 9–20 K. These values were corrected to $S = 10$ ($g = 2$) as shown previously.[21] The temperature corresponding to the maximum peaks in χ''_m of complex **1** (*cf.* Fig. 3) is almost equal to that for complex **2** at the same frequency. The temperature corresponding to the χ''_m maximum peaks is lower in complex **3** (6.3 K) than in complexes **1** and **2** (6.8 K) at a frequency of 1340 Hz. This shows that the rate of the resonant magnetization tunneling (RMT) in complex **3** is higher than that found in complexes **1** and **2**. The difference between the hysteresis loops of complexes **1**, **2** and **3** also confirms this fact.[10] We can thus conclude that complexes **1**, **2** and **3** do indeed have different relaxation processes.

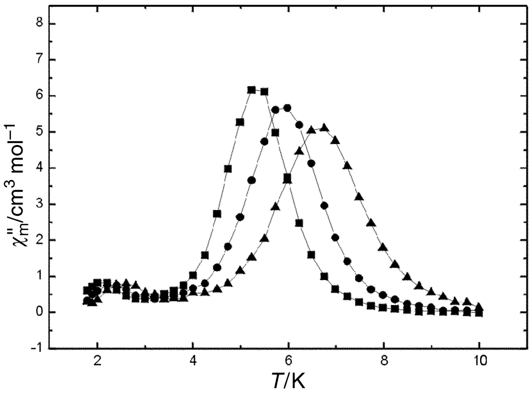

Fig. 3 Plot of the out-of-phase AC magnetic susceptibility, χ''_m, *vs.* temperature for a polycrystalline sample of complex **1**. Data were collected with the 1.0 Oe AC field oscillating at three frequencies: (■) 100 (●) 332 (▲) 1340 Hz.

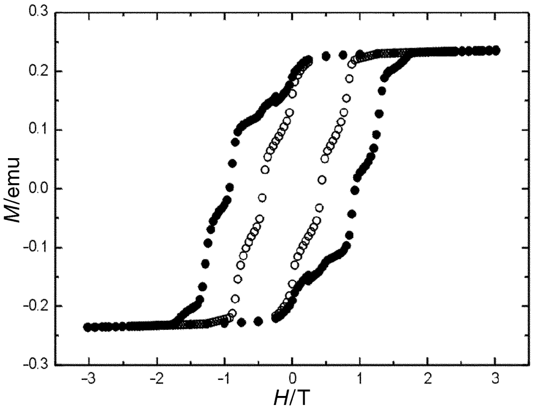

Fig. 4 Magnetic hysteresis loops of complex **1** measured at 2.2 (●) and 2.6 K (○) for a polycrystalline sample.

Hysteresis effects. Fig. 4 shows the magnetic hysteresis loops of complex **1** with the magnetic field applied at temperatures of 2.2 and 2.6 K. As the field strength was increased, so steps appeared. In addition, the number of steps increased with decreasing temperature. Five and three steps were observed at 2.2 and 2.6 K, respectively and more could probably be seen at lower temperature.

First derivative plots for the two magnetic hysteresis loops in complex **1** highlight the position of the steps (*cf.* Fig. 5). Five maxima for the 2.2 K plot are clearly visible. The period maxima appear every 0.41 T. Similarly, the plot for complex **1** at 2.6 K shows three corresponding steps. Coercivity values increased with decreasing temperature, *e.g.* 0.44 T at 2.6 K and 0.92 T at 2.2 K for complex **1**.

For complex **2**, similar magnetic hysteresis loops were obtained, showing five and three steps at 2.2 and 2.6 K, respectively. Complex **2** has a relatively large coercivity value (1.03 T) at 2.2 K.

The steps in the magnetic hysteresis loops for Mn12 compounds are related to an increase in the rate of the magnetiz-

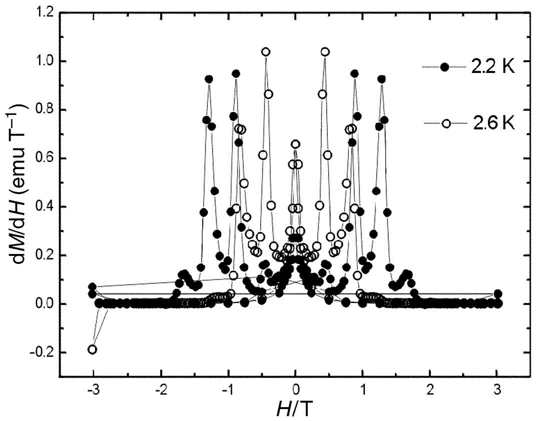

Fig. 5 First derivative plots corresponding to the 2.2 (●) and 2.6 K (○) magnetic hysteresis loops of complex **1**.

Table 2 Mn12 compounds included in the Cambridge Structural Database for which the largest number of steps in the magnetic hysteresis loops is known. The arrangement of best planes through the four Mn(IV) and eight Mn(III) atoms relative to each other is compared

Name	Steps	Arrangement	T/K	Ref.
AQACMN	7	Co-planar	1.7	2, 14
Complex **1**	5	Co-planar	2.2	This work
Complex **2**	5	Co-planar	2.2	This work
RUHSES	5	Non-co-planar	1.9	8
WIMRIT	4 (1)	Non-co-planar	1.85	11 (13)
RUQMAR	3	Co-planar	1.5	23
RUHSIW	3	Non-co-planar	1.9	8
NORXUM	3	Non-co-planar	2.0	9
KEQXEQ	2	Non-co-planar	1.4	10
YOFGAB	1	Non-co-planar	2.2	13

ation coming from so-called resonant magnetization tunneling (RMT).[3]

When increasing the field from zero to +3 T after saturation, seven maxima were observed in the magnetic hysteresis loops within the temperature range (down to 1.7 K) for the neutral Mn12Ac, including the step at zero field. Compared to the five and three steps for the analogues **1** and **2**, other studies have always reported less than five steps (with the exception of Aubin *et al.*,[8] who reported five steps).[9–11,13,23] Comparing complex **3** to **1** and **2**, its magnetic hysteresis loop has a larger slope at zero field.

The question thus arises: What chemical factors could influence the number of steps and the slope in the magnetic hysteresis loops for the Mn12 compounds? Certainly, for Mn12 compounds containing different ligands, different magnetic hysteresis loops are observed. Even solvents have an influence on the number of steps in the magnetic hysteresis loop and the rate of resonant magnetization tunneling.[7]

Other possible factors are the molecular and crystal structures. However, the crystal packing appears not to play a role, as Gatteschi *et al.*[1] found that all evidence points to the phenomena being associated with the individual clusters. Also, the distances between neighboring manganese ions are so long (~7 Å) that magnetic interactions are negligible.[2] Furthermore, crystal and molecular structure determinations are usually performed at temperatures much higher than the temperatures at which the measurement of the hysteresis loops take place. Thus, the packing found in the crystal structure as well as the molecular structure at the temperature of the X-ray diffraction experiment may differ from that found in the crystal at the temperature of the magnetic hysteresis experiment. Nevertheless, the molecular structure, in particular the relative positioning of the twelve manganese atoms, may hold a clue to the magnetic properties. A careful study of the Mn12 compounds included in the Cambridge Structural Database[24] for which hysteresis loops are available (*cf.* Table 2) suggests that if the best plane through the four Mn(IV) atoms and the best plane through the eight Mn(III) atoms are co-planar, in general, a larger number of steps in the hysteresis loops is likely to be observed. In complexes **1** and **2**, where five steps were found at 2.2 K, the best planes through the two sets of Mn atoms were indeed found to be co-planar. It is thus possible that at lower temperatures, even more steps may be observed.

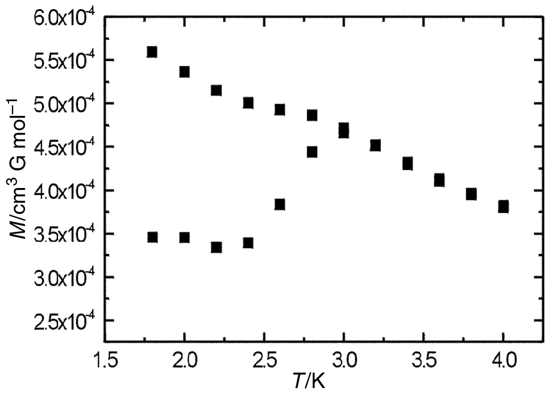

Fig. 6 The zero-field-cooled (ZFC) and field-cooled (FC) data for a polycrystalline sample of complex **1**.

The hysteresis loop observed for complex **3** has a larger slope at zero field, as compared to **1** and **2**. The origin of this behaviour for complex **3** requires future investigation.

Zero-field-cooled (ZFC) and field-cooled (FC) magnetization. The zero-field-cooled (ZFC) and field-cooled (FC) data for a polycrystalline sample of complex **1** are shown in Fig. 6. There is a difference in the zero-field-cooled (ZFC) and the field-cooled (FC) magnetization for both complexes. The slow relaxation of the magnetization is probably responsible for the large difference between the ZFC and FC magnetization data.

For complex **1** (*cf.* Fig. 6), the ZFC and FC magnetization curves become superimposed at 3.0 K. The same result was obtained for $[Mn_{12}O_{12}(EtCO_2)_{16}(H_2O)_3]\cdot H_2O$,[13] whereas in complex **3**, the curves became identical at 3.4 K. All these facts indicate a relaxation process at *ca.* 3.0 K.

Acknowledgements

This project was supported by the National Natural Science Foundation of China (29831010, 20023005), State Key Project of Fundamental Research of China (1998061306), the Claude Harris Leon Foundation and the National Research Foundation of South Africa. The authors wish to thank M.W. Esterhuysen for his valuable contribution to the crystal structure determinations and P. F. M. Verhoeven for infrared analyses.

References

1 D. Gatteschi, A. Caneschi, L. Pardi and R. Sessoli, *Science*, 1994, **265**, 1054.
2 J. R. Friedman, M. P. Sarachik, J. Tejada and R. Ziolo, *Phys. Rev. Lett.*, 1996, **76**, 3830.
3 J. M. Hernandez, X.-X. Zhang, F. Luis, J. Bartolome, J. Tejada and R. Ziolo, *Europhys. Lett.*, 1996, **35**, 301; J. M. Hernandez, X.-X. Zhang, F. Luis, J. Tejada, J. R. Friedman, M. P. Sarachik and R. Ziolo, *Phys. Rev. B: Condens. Matter*, 1997, **55**, 5858.
4 E. M. Chudnovsky and D. A. Garanin, *Phys. Rev. Lett.*, 1997, **79**, 4469.
5 A. D. Kent, Y.-C. Zhong, L. Bokacheva, D. Ruiz, D. N. Hendrickson and M. P. Sarachik, *Europhys. Lett.*, 2000, **49**, 521; L. Bokacheva, A. D. Kent and M. A. Walters, *Phys. Rev. Lett.*, 2000, **85**, 4803.
6 W. Wernsdorfer, T. Ohm, C. Sangregorio, R. Sessoli, D. Mailly and C. Paulsen, *Phys. Rev. Lett.*, 1999, **82**, 3903; X.-X. Zhang, J. M. Hernandez, E. del Barco, J. Tejada, A. Roig, E. Molins and K. Wieghardt, *J. Appl. Phys.*, 1999, **85**, 5633.

7 L. Thomas, F. Lionti, R. Ballou, D. Gatteschi, R. Sessoli and B. Barbara, *Nature*, 1996, **383**, 145; E. M. Chudnovsky, *Science*, 1996, **274**, 938.

8 S. M. J. Aubin, Z.-M. Sun, I. A. Guzei, A. L. Rheingold, G. Christou and D. N. Hendrickson, *Chem. Commun.*, 1997, 2239.

9 D. Ruiz, Z. M. Sun, B. Albela, K. Folting, J. Ribas, G. Christou and D. N. Hendrickson, *Angew. Chem., Int. Ed.*, 1998, **37**, 300.

10 J. An, Z.-D. Chen, J. Bian, J.-T. Chen, S.-X. Wang, S. Gao and G.-X. Xu, *Inorg. Chim. Acta*, 2000, **299**, 28.

11 S. M. J. Aubin, S. Spagna, H. J. Eppley, R. E. Sager, G. Christou and D. N. Hendrickson, *Chem. Commun.*, 1998, 803.

12 S. M. J. Aubin, Z.-M. Sun, L. Pardi, J. Krzystek, K. Folting, L. C. Brunel, A. L. Rheingold, G. Christou and D. N. Hendrickson, *Inorg. Chem.*, 1999, **38**, 5329.

13 H. J. Eppley, H. L. Tsai, N. D. Vries, K. Folting, G. Christou and D. N. Hendrickson, *J. Am. Chem. Soc.*, 1995, **117**, 301.

14 T. Lis, *Acta Crystallogr., Sect. B*, 1980, **36**, 2042.

15 COLLECT, Data Collection Software, Nonius BV, Delft, The Netherlands, 1998.

16 Z. Otwinowski and W. Minor, *Methods Enzymol.*, 1997, **276**, 307.

17 G. M. Sheldrick, SHELX-97, Program for Crystal Structure Analysis, Univ. of Göttingen, Germany, 1997.

18 L. J. Farrugia, *J. Appl. Crystallogr.*, 1999, **32**, 837.

19 L. J. Farrugia, *J. Appl. Crystallogr.*, 1997, **30**, 565.

20 C. W. Dwiggins, *Acta Crystallogr., Sect. A*, 1975, **31**, 146.

21 R. Sessoli, H.-L. Tsai, A. R. Schake, S.-Y. Wang, J. B. Vincent, K. Folting, D. Gatteschi, G. Christou and D. N. Hendrickson, *J. Am. Chem. Soc.*, 1993, **115**, 1804.

22 Z.-M. Sun, D. Ruiz, E. Rumberger, C. D. Incarvito, K. Folting, A. L. Rheingold, G. Christou and D. N. Hendrickson, *Inorg. Chem.*, 1998, **37**, 4758.

23 Y.-G. Wei, S.-W. Zhang, M.-C. Shao and Y.-Q. Tang, *Polyhedron*, 1997, **16**, 1471.

24 F. H. Allen and O. Kennard, *Chem. Des. Autom. News*, 1993, **8**, 1; F. H. Allen and O. Kennard, *Chem. Des. Autom. News*, 1993, **8**, 31.